Integrative Cancer Therapies
Volume 24: 1–14

DOI: 10.1177/15347354251335599
journals.sagepub.com/home/ict
Sage

Cytotoxic Potential and Metabolomic Profiling of *Solanum lycopersicum* Roots Extract and Their Nanocrystals: An *In Silico* Approach

Marwa A. M. Abdel-Razek, MSc[1*], Miada F. Abdelwahab, PhD[1,2*], Soad A. Mohamad, PhD[3], Hesham A. Abou-Zied, PhD[4], Usama R. Abdelmohsen, PhD[1,5], and Ashraf N. E. Hamed, PhD[1,2]

Abstract

Solanum lycopersicum L. Moench (Tomato) is a rich source of bioactive compounds. This study investigated the anticancer potential of *S. lycopersicum* roots methanol extract (TMESLR) and their nanocrystals (TMESLR-NCs) against breast (MCF-7), hepatocellular (HepG2), and colon (Caco-2) cancer cell lines, for the first time. TMESLR exhibited significant cytotoxicity against all 3 cell lines, with the nanocrystals demonstrating enhanced activity, Caco-2, MCF-7, and HepG2 cells with IC_{50} values of 9.69 ± 0.6, 12.52 ± 0.58, and 14.34 ± 0.62 µg/mL, respectively. Whereas, the prepared TMESLR-NCs displayed significantly the highest cytostatic potential against Caco-2 with IC_{50} value of 5.733 ± 0.29 µg/mL. Metabolomic profiling revealed **17** secondary metabolites, including flavonoids, phenolic acids, and terpenoids. *In silico* analyses, including PPI network construction, GO enrichment, and KEGG pathway analysis, highlighted the involvement of apoptotic pathways, p53 signaling, and TNF signaling in the anticancer effects of TMESLR. Molecular docking studies identified chlorogenic acid and inosine as potential inhibitors of Histone Deacetylase 2 (HDAC2). Inosine (**6**) displayed a superior docking score of −7.86 kcal/mol, interacting with critical residues GLY154, ASP269, and HIS146. On the other hand, chlorogenic acid (**12**) achieved a docking score of −7.32 kcal/mol, forming stable interactions with TYR308, PHE210, and LEU276 residues. These findings suggest that TMESLR and TMESLR-NCs possess promising anticancer activity and warrant further investigation as potential therapeutic agents.

Keywords

cytotoxicity, HPLC-HESI-HRMS, molecular docking, nanocrystals, *Solanum lycopersicum* (syn.: *Lycopersicum esculentum*)

Received: January 11, 2025; accepted: April 2, 2025

Introduction

Cancer is the second greatest cause of death globally and a serious public health concern.[1] It is prompted by abnormal processing of genetic information, due to mutations affecting tumor suppressor genes and oncogenes, or altered epigenetic pathways resulting in chromatin structural abnormalities that are either localized or global.[2] The dysregulated expression of several histone methyltransferases is a major cause of changes in the epigenetic landscapes of cancer cells. The pathogenesis of colorectal, breast, esophageal squamous cell carcinoma, hepatocellular carcinoma, and melanoma has been associated with changes in the expression or activity of G9a, Setdb1, Smyd2, or PR-SET7 methyltransferases.[3]

Interestingly, the innovative and developing field of nanobiotechnology is tremendously useful in the biomedical industry. Drug nanocrystals are molecular assemblies that can be combined to generate the drug in a crystalline form enclosed in a thin stabilizer layer. Nanocrystals technology is a remarkable alternative to the existing nanocarrier drug delivery mechanisms in enhancing[4] the bioavailability of medications which are not freely soluble in water.[5] Because of their small size (350-500 nm), they usually exhibit noteworthy biological and physicochemical activities that are different from those of larger particles.[6] They have exceptionally shown significant potential in cancer treatments,[7] orthopedics,[8] and dentistry.[9] Nanocrystal formulation can be used to improve drug delivery, targeting

and bioavailability. It is possible to administer the drug orally or intravenously and the limited carrier, which mostly consists of a thin layer of surfactant may greatly reduce any toxicity.[10]

Natural products have been evidenced as a source for developing new and effective therapeutic agents. Modern equipment in isolation, structure elucidation and identification of natural products, as well as the use of updated software and databases, give a great opportunity in screening natural products as forceful lead molecules. This has evolutionally confirmed their paramount role in drug discovery.[11-15]

Likewise, *S. lycopersicum*, belonging to family Solanaceae, has shown powerful antioxidant efficacy in addition to cardiovascular protection, anticancer, anti-inflammatory, antimicrobial, antiviral, neuroprotection, antidiabetic, radioprotective and gut modulating activities.[16] The main reason for this biological diversity was attributed to the active metabolites, including caretonoids, alkaloids, flavonoids, and steroidal derivatives.[16] Furthermore, various secondary metabolites comprising flavonoids and phenolic acids, in addition to lycopene and β-carotene are abundant in *S. lycopersicum* seeds and roots. Tomato is a model vegetable crop with a vast array of valuable phytochemicals and biological uses.[16]

In previous investigations, the seeds, fruits as well as the leaves of *S. lycopersicum* were extensively studied, Whereas the roots, that are considered as plant by-products, are underexplored parts. Therefore, the present research work aimed to investigate the cytotoxic efficacy of the TMESLR and TMESLR-NCs against 3 distinct cancer cell lines (Caco-2, MCF-7, and HepG2). Moreover, the TMESLR chemical profile was investigated through metabolomic analysis. Finally, the study involved protein-protein interaction network construction, gene ontology analysis as well as molecular docking for the dereplicated metabolites, with the purpose to comprehend the gene functions and molecular pathways associated with the bioactive compounds, as potential therapeutic agents against cancer.

Materials and Methods

Plant Material

In March 2022, 500 g of the fresh *S. lycopersicum* roots were taken from a farm in Maghagha city, Minia, Egypt, with the owner's consent. Prof. Nasser Barakat (Department of Botany and Microbiology, Faculty of Science, Minia University) identified the plant. **Mn-Ph-Cog-061** is the voucher number of the plant under study was kept in Herbarium of Department of Pharmacognosy, Faculty of Pharmacy, Minia University, Minia, Egypt.

Chemicals and Reagents

Ethanol, Formic acid (Merck, Germany), petroleum ether (Merck, Germany), methanol (99.8%) and DMSO (El-Nasr Company for Pharmaceuticals and Chemicals, Egypt), Insulin, acetonitrile, and 1% penicillin-streptomycin, Staurosporine® (Sigma-Aldrich, Germany), 10% FBS (Hyclone, USA), and DMEM high glucose (Invitrogen/Life Technologies, USA).

Extraction

The collected *S. lycopersicum* roots were dried in shade for 2 weeks. Afterward, they were grinded into fine powder resulting in a total amount of 55 g. The resulted fine powder was extracted using 99.8% methanol (1 L, 3×, 2 weeks interval). TMESLR was then evaporated using rotary evaporator (Heidolph®, Germany). The yielded viscous pale green TMESLR (5 g). It was kept in the refrigerator until further processing.

Cytotoxic Activity Assay

The antiproliferative potential of TMESLR and their prepared nanocrystals was evaluated, implementing the MTT assay.[17,18] The cancer cell lines utilized in this test were previously obtained from the American Type

[1]Department of Pharmacognosy, Faculty of Pharmacy, Minia University, Minia, Egypt
[2]Department of Pharmacognosy, Faculty of Pharmacy, Minia National University, New Minia, Egypt
[3]Department of Pharmaceutics and Clinical Pharmacy, Faculty of Pharmacy, Deraya University, Universities Zone, New Minia City, Egypt
[4]Department of Medicinal Chemistry, Faculty of Pharmacy, Deraya University, Universities Zone, New Minia City, Egypt
[5]Deraya Center for Scientific Research, Deraya University, Universities Zone, New Minia, Egypt

*These authors contributed equally to this work.

Corresponding Authors:
Usama R. Abdelmohsen, Deraya Center for Scientific Research, Deraya University, Universities Zone, 61111 New Minia, Egypt.
Email: usama.ramadan@mu.edu.eg

Ashraf N. E. Hamed, Department of Pharmacognosy, Faculty of Pharmacy, Minia University, Minia 61519, Egypt and Department of Pharmacognosy, Faculty of Pharmacy, Minia National University, New Minia, Egypt.
Email: ashrafnag@mu.edu.eg

Marwa A. M. Abdel-Razek, Department of Pharmacognosy, Faculty of Pharmacy, Minia University, Minia 61519, Egypt.
Email: drmarwaali33@gmail.com

Culture Collection (Manassas, VA, USA). They comprised Caco-2 (RRID: CVCL_0025), MCF-7 (RRID: CVCL_0031) and HepG2 (RRID: CVCL_0027) cell lines. First, the cells were cultured at 37°C and 5% CO_2 in DMEM high glucose (Invitrogen/Life Technologies, USA) with 10% FBS (Hyclone, USA), 1% penicillin-streptomycin, and 10 mg/mL of insulin. After that, they were transferred to 96-well plates and incubated for the entire night at densities of 2.2 and 104 cells/cm^2. Subsequently, the growing cells were exposed to TMESLR at diverse concentrations (20, 30, 40, 50, and 60 mg/mL) dissolved in DMSO. The following day, the cell viability was evaluated using the MTT assay, as formerly described by Hamed et al.[17]

Preparation of TMESLR-NCs

TMESLR-NCs were prepared by dissolving a specified amount of TMESLR in absolute ethanol and petroleum ether mixture 25:75 ratio. The final amount achieved 50 mg/5 mL solution was well sonicated in an ultrasonicate bath at a frequency of 50 kHz (Branson® Ultrasonic Bath,). Tween 80 surfactant (the reported toxicity effect of tween 80 according to previous literature is 1 mg/mL while the concentration used in this formulation is 0.02 mg/mL that had not cytotoxic effect)[19] was added. After that, the mixture was stirred for 15 min at 1000 rpm. For solvent evaporation, the resultant solution was put on a BUCHI Rotavapor™ R-300 rotary evaporator. The resultant powder was kept at −20°C after being collected as TMESLR-NCs.[7-9]

Particle Size (nm) and Size Distribution

Photon correlation spectroscopy was utilized to ascertain the size distribution and particle size of the prepared particles in terms of average volume diameters and polydispersity index. Dynamic Light Scattering (DLS) particle size analyzer (Zetasizer Nano ZN, Malvern Panalytical Ltd, UK) was used at a fixed angle of 173° at 25°C. Three examinations of the sample were conducted.[5]

Scanning Electron Microscopy (SEM)

High-resolution SEM was performed to investigate the nanocrystals morphology. The samples were diluted (1:10) in ultrapure water, then 20 µL of slurries were spread on amorphous polycarbonate grids and left to dry at 25°C. They were extra dried using CO_2, sputter coated with gold in a metallizer and examined under a SEM with accelerating voltage at 200 kV.[20]

The produced nanocrystals' morphology was examined using a SEM device (SEM, TESCAN, Warrendale, PA). This was accomplished by placing the nanoparticle powder on stubs and covering them with a layer of gold.

LC-MS Metabolomic Analysis

A 6530 Q-TOF LC-MS (Agilent Technologies, Japan) equipped with an autosampler (G7129A), a Quat pump (G7104C), and a Column Comp (G7116A) for chromatographic separation were used at the Faculty of Pharmacy, Fayoum University, to perform metabolomic profiling of TMESLR. An Agilent Technologies Zorbax RP-18 column (150 mm × 3 mm, dp = 2.7 µm) was used to separate the analytes. The mass spectra were obtained using ESI in both positive and negative ionization modes with a capillary voltage of 4500 V. They were captured between 50 and 3000 m/*z*. The temperature of the drying gas was 200°C, and the flow rate was 8 mL/min. The collision energy was set at 10 V, while the fragmentator and skimmer voltages were set at 130 and 65 V, respectively. The Phenomenex Kinetex 2.6 mm XB-C18 150 mm × 4.6 mm column, which was maintained at 30°C and connected to a guard column, was filled with 10 mL of samples (1 mg/mL in methanol). For the mobile phase, a mixture of acetonitrile (B) and LC-MS grade water (A) with 0.1% formic acid each was used. The gradient elution proceeded from 5% to 20% B in 2 min, 20% to 98% B in 18 min, 98% B in 5 min, and finally 98% to 5% B in 2 min, all while maintaining a flow rate of 500 µL/min. Capillary temperature (320°C), spray voltage (+3.5 or −2.7 kV), sheath gas (57.50 Pa), sweep gas (3.25 Pa), auxiliary gas (16.25 Pa), probe heater (462.50°C), AGC target (1e6), S-Lens RF (50 cm) resolution (70.000), and microscans (1) were the MS parameters used for the HPLC-HESI-HRMS analysis. The raw data was converted into positive and negative files in the mz/mL format using ProteoWizard after a variance analysis of the MS data was obtained using Mzmine 2.12. Lastly, metabolite identification was accomplished by referring to the metabolite database (METLIN 2020) and Dictionary of Natural Products (DNP 2020) databases.[21,22]

In Silico Study

Protein-Protein Interaction (PPI) Network Analysis. To explore the interactions between the bioactive secondary metabolites tentatively identified in our study and their protein targets, we utilized the STITCH database.[23] This platform facilitated the investigation of compound-protein interactions, integrating data from sources such as GEO and PharmGKB. This study was able to better understand the molecular mechanisms behind the metabolites effects by mapping these interactions, which also highlighted the metabolites' potential as therapeutic agents in the treatment of cancer.[24] To better recognize the cytotoxic and anticancer effects of the bioactive compounds identified in TMESLR, the STRING database was utilized for constructing (PPI) networks.[25] Only interactions with a confidence score above 0.4 were included to ensure robustness and

reliability. The networks were analyzed and visualized using Cytoscape software, with the CytoHubba plugin was employed to identify central molecular targets relevant to anticancer activity.[26] This analysis highlighted critical proteins and molecular pathways, providing insights into the therapeutic potential of these compounds for cancer management.

Gene Ontology (GO) and KEGG Pathway Analysis. Gene Ontology (GO) and Kyoto Encyclopedia of Genes and Genomes (KEGG) pathway enrichment analyses were performed in order to obtain a better understanding of the molecular mechanisms linked to the cytotoxic effects of TMESLR compounds. These analyses elucidated 3 critical dimensions: Biological Processes (BP), focusing on cancer progression; Cellular Components (CC), pinpointing the loci of activity within cells, and Molecular Functions (MF), detailing specific molecular interactions. The Shiny GO platform (v0.80.) was utilized for this analysis, applying a False Discovery Rate (FDR) threshold of less than 0.05 to ensure statistical significance.[27] Results were visualized using enrichment bubble plots created by SRplot (v1.0.).[28] This comprehensive approach provided valuable insights into the gene functions and pathways associated with the bioactive compounds, underscoring their potential as therapeutic agents against cancer.

Molecular Docking Studies. The binding relationships between bioactive tentatively secondary metabolites from TMESLR and important proteins implicated in cancer processes were examined using molecular docking simulations. These investigations sought to investigate putative molecular anticancer mechanisms and validate the projected molecular targets. The RCSB Protein Data Bank (https://www.rcsb.org/) provided pertinent protein structures, preprocessed to remove non-essential molecules, and optimized with necessary modifications such as the addition of hydrogen atoms and charges. Docking experiments were conducted using the Discovery Studio Client platform (v.16.),[29] revealing promising binding interactions between the tentatively identified compounds and target proteins involved in cancer cell proliferation and survival. This analysis provided a foundation for further exploration of these compounds as potential anticancer agents.

Statistical Analyses

The mean ± standard error of mean was used to display the data. Tukey-Kramar post-analysis testing is performed after one-way analysis of variance (ANOVA). Graph Pad Prism 7 (Graph Pad Software, San Diego, California, USA) was used for statistical calculations. The results were estimated significant when $P < 0.05$.

Results

Cytotoxic Activity Assay

The MTT viability assay was used to examine the cytotoxic activity of TMESLR, with Staurosporine®, an anticancer medication, serving as the positive control. Several cancer cell lines (Caco-2, MCF-7, and HepG2) were used in this assay. The findings demonstrated that TMESLR had a significant level of inhibitory activity against Caco-2, MCF-7, and HepG2 cells, with respective IC_{50} values of 9.69 ± 0.6, 12.52 ± 0.58, and 14.34 ± 0.62 µg/mL. While, the TMESLR-NCs showed higher cytotoxic activity especially against Caco-2, and HepG2 with IC_{50} value of 5.733 ± 0.29, and 12.08 ± 0.56 µg/mL, respectively, demonstrating an enhanced cytotoxic activity for the TMESLR. While, the growth of MCF-7 cell line was inhibited at IC_{50} value of 20.91 ± 1.22 µg/mL as described in Table 1.

Characterization of Nanocrystals

The TMESLR-NCs displayed a mean particle size of 570 ± 25 nm and a poly dispersity index value of 0.2 to 0.5 indicating a narrow size distribution. The data of particle size distribution relative to their PI were presented in Figure 1 that enhance the bioavailability, in addition to zeta potential -23 ± 4.9 mV indicating high stability.[30,31,53] SEM results Figure 2 approved different particle sizes distribution and showed that the nanocrystals had grouped quasispheroidal within the sample.[32]

Metabolomic Study

The metabolomic profile of TMESLR revealed different varieties of chemical classes. Supplemental Table S1 as well as Figures 3-5 are illustrating the secondary metabolites that were tentatively identified through metabolic profiling of TMESLR utilizing the untargeted HPLC-HESI-HRMS metabolomics technique. In reference to (DNP 2020) and (METLIN 2020) databases,[21,22] the mass ion peak at *m/z* 165.0792 $[M+H]^+$ for the anticipated molecular formula $C_{10}H_{16}$ was dereplicated as coumaric acid (**1**), a phenolic acid previously identified from the crushed *S. lycopersicum* seeds.[33] An acidic derivative was characterized as azelaic acid (**2**), with regard to the molecular formula $C_9H_{16}O_4$ and the mass ion peak at *m/z* 189.1164 [M+H]+.[33] Whereas, the mass ion peak at *m/z* 199.1367 $[M+H]^+$ was dereplicated as syringic acid (**3**) in compliance with the molecular formula $C_9H_{10}O_5$, also formerly identified in the crushed *S. lycopersicum* seeds.[33] Compound (**4**) was identified as resveratrol in agreement with the mass ion peak at *m/z* 229.1155 $[M+H]^+$ and the molecular formula $C_{14}H_{12}O_3$ which was previously reported as a stilbene metabolite in *S. lycopersicum* fruits.[34] Moreover, the mass ion peak at *m/z* 235.1621 $[M+H]^+$ for the suggested molecular formula $C_{16}H_{26}O$ was dereplicated

Table 1. Cytotoxic activities of TMESLR, and its nanocrystals.

	IC_{50} values (mean ± S.E.M; µg/mL)		
Sample	Caco-2	MCF-7	HepG2
TMESLR	9.69 ± 0.6*	12.52 ± 0.58	14.34 ± 0.62
TMESLR-NCs	5.733 ± 0.29*	20.91 ± 1.22	12.08 ± 0.56*
Staurosporine®	3.148 ± 0.16*	8.1454 ± 0.47*	4.408 ± 0.21*

Values represent Mean ± SEM using one-way ANOVA test followed by Tukey-Kramer test.
*Very significant difference compared with the corresponding Staurosporine® IC_{50} values (P<0.05).

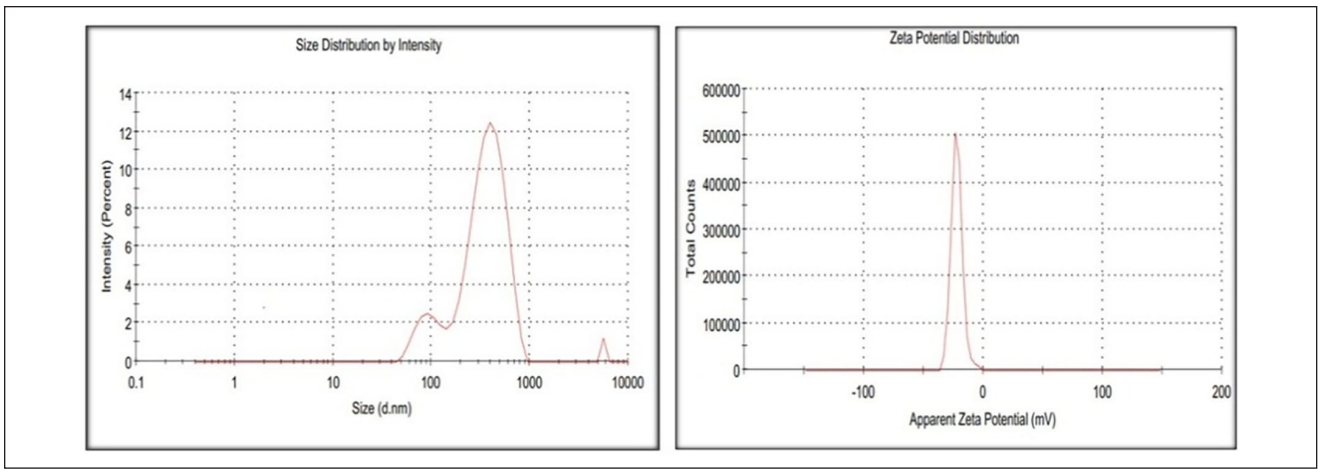

Figure 1. Mean particle size (left) and zeta potential of nanocrystals suspensions (right).

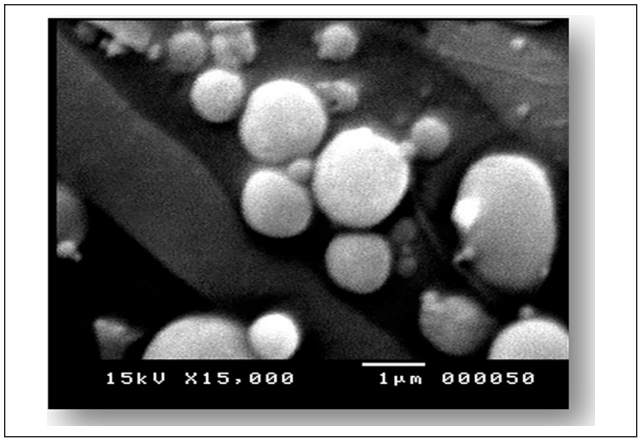

Figure 2. SEM images of TMESLR nanocrystals with power of magnification (15 KV×3.500).

as 2,6,10,14-hexadecatetraen-1-ol (**5**); an alcoholic derivative that was earlier purified from *S. lycopersicum* fruits.[35] A nucleoside derivative was dereplicated according to the molecular formula $C_{10}H_{12}N_4O_5$ and the mass ion peak at *m/z* 267.1679 $[M\text{-}H]^-$, as inosine (**6**) that was previously reported in the crushed *S. lycopersicum* seeds.[33] A diterpene derivative was also characterized as phytol (**7**), corresponding to the molecular formula $C_{20}H_{40}O$ and the mass ion peak at *m/z* 295.2351 $[M\text{-}H]^-$. It was earlier identified from the crushed leaves of *S. lycopersicum*.[36] The mass ion peak at *m/z* 301.2248 $[M\text{-}H]^-$ and the molecular formula $C_{15}H_{10}O_7$ were dereplicated as quercetin (**8**); a flavanol that was previously identified in *S. lycopersicum* seeds.[33] Another diterpene derivative was identified in line with the mass ion peak at *m/z* 303.2401 $[M\text{-}H]^-$ and the molecular formula $C_{20}H_{32}O_2$, as lycosantalonol (**9**), which was formerly obtained from *S. lycopersicum* leaves.[33] Moreover, the mass ion peak at *m/z* 309.1379 $[M+H]^+$ and the molecular formula $C_{17}H_{12}N_2O_4$ were dereplicated as flazin (**10**), an indole alkaloid that was previously isolated from *S. lycopersicum* fruits.[37] Compound (**11**) was dereplicated as dihydromyricetin (flavanol) in agreement with the mass ion peak at *m/z* 321.1854 $[M+H]^+$ and the molecular formula $C_{15}H_{12}O_8$. It was earlier purified from the *S. lycopersicum* fruits.[38] Chlorogenic acid (**12**) was dereplicated in accordance with the molecular formula $C_{16}H_{18}O_9$ and the mass ion peak at *m/z* 355.2778 $[M+H]^+$, this phenolic acid was previously obtained from *S. lycopersicum* seeds.[33] The vitamin δ-tocopherol (**13**) was dereplicated based on the molecular formula $C_{27}H_{46}O_2$ and the mass ion peak at *m/z* 401.2982 $[M\text{-}H]^-$, this vitamin was formerly

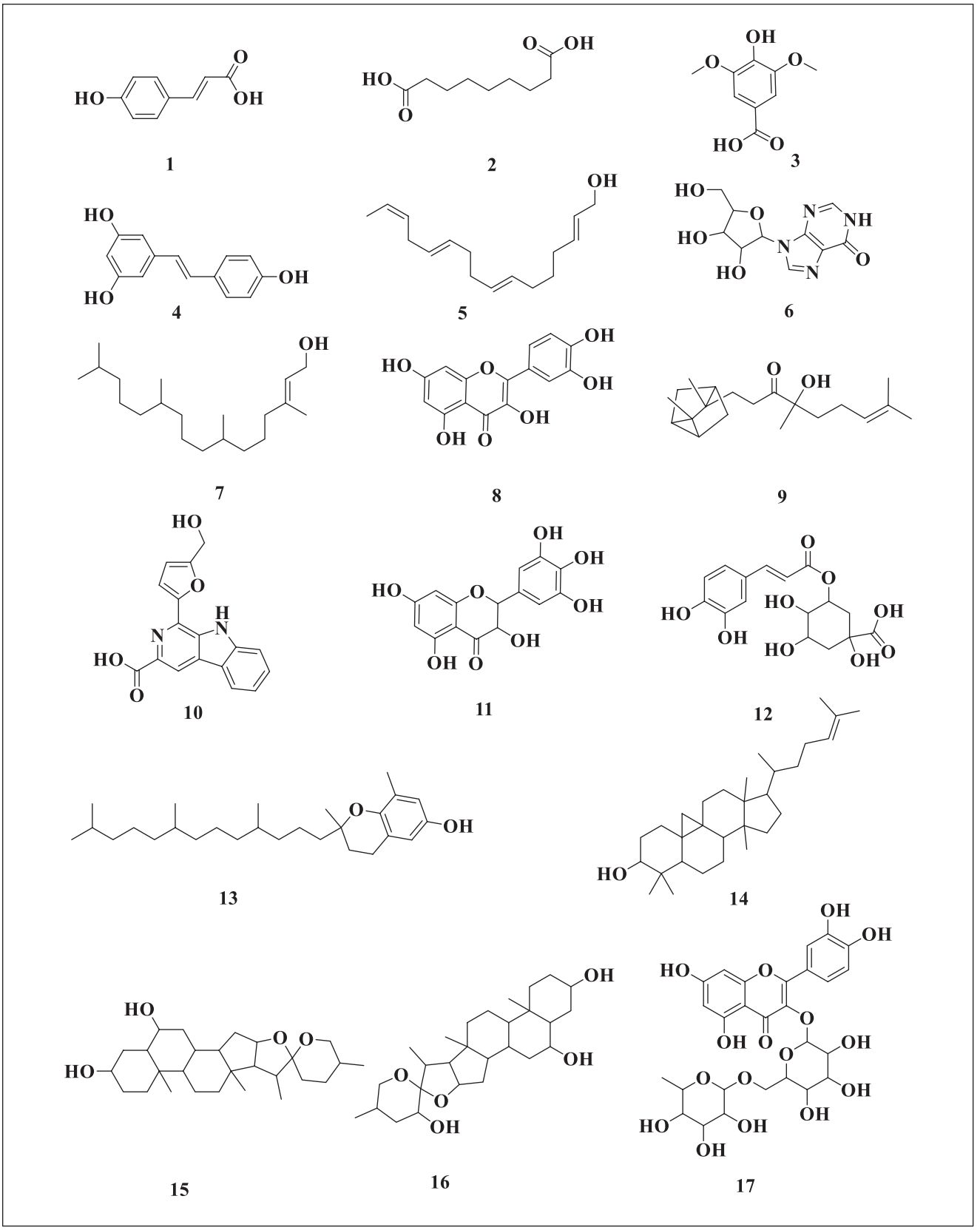

Figure 3. Chemical structures of the tentatively characterized metabolites from TMESLR.

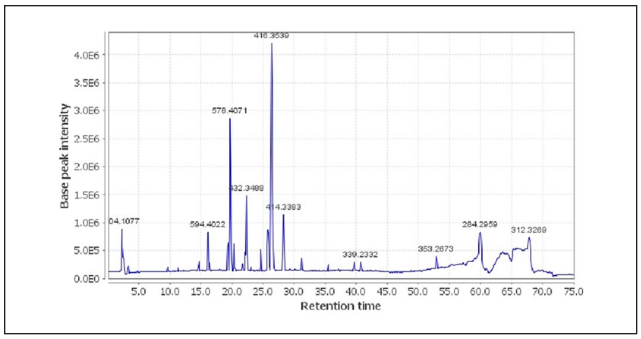

Figure 4. Positive total ion chromatogram of TMESLR.

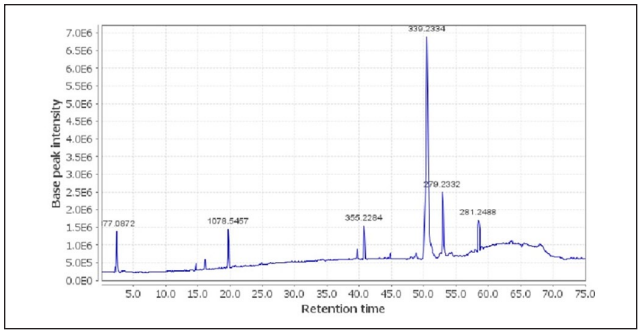

Figure 5. Negative total ion chromatogram of TMESLR.

identified in *S. lycopersicum* fruits.[39] The mass ion peak at *m/z* 425.1934 $[M-H]^-$ for the estimated molecular formula $C_{30}H_{50}O$ was characterized as cycloartenol (**14**); a triterpenoidal derivative, which was earlier isolated from *S. lycopersicum* seeds.[33] Compounds (**15** and **16**) were dereplicated as neochlorogenin and hispigenin (steroidal saponin), respectively, in agreement with the mass ion peaks at *m/z* 431.1998 and 447.1585 $[M-H]^-$ and the molecular formulae $C_{27}H_{44}O_4$ and $C_{27}H_{44}O_5$, they were previously identified in *S. lycopersicum* seeds.[33] Finally, a flavonol derivative with mass ion peaks at *m/z* 609.5092 $[M-H]^-$ was identified as rutin (**17**),which was also previously reported in tomato seeds.[33]

In Silico Studies

Identifying Therapeutic Targets for Cancer Treatment. Protein targets were identified using NCBI-GEO and PharmGKB databases to ensure relevance to Caco-2, MCF-7, and HepG2 cancer models.[40,41] NCBI-GEO datasets with at least 50 tumor and 50 normal samples were selected, and differential gene expression analysis was performed using GEO2R and the limma package, applying a cutoff of $\log2FC \geq \pm 1.5$, and $FDR < 0.05$.[42] Only genes consistently altered across at least 3 independent datasets were included. PharmGKB was used to filter cancer-related protein targets based on gene-drug interactions, prioritizing those involved in apoptosis, p53 signaling, TNF, NF-κB, and epigenetic regulation (eg, HDAC2, CASP3, BCL2, FASLG, and TNF). The final 73 (Supplemental Table S2) selected protein targets were mapped using STRING for protein-protein interaction (PPI) analysis,[43] followed by Gene Ontology (GO) enrichment and molecular docking studies to assess their interactions with bioactive compounds tentatively identified in TMESLR.[44]

STITCH database analysis of TMESLR compounds and cancer targets. To explore the interactions between the key bioactive compounds tentatively identified from TMESLR; such as coumaric acid (**1**), syringic acid (**3**), resveratrol (**4**), inosine (**6**), quercetin (**8**), chlorogenic acid (**12**), and rutin (**17**), and the identified protein targets, we utilized the STITCH database. This comprehensive analysis mapped the interactions between the compounds and proteins cataloged in the GEO and PharmGKB datasets Figure 6. The findings highlighted the potential of these compounds to act synergistically, revealing intricate interaction networks that contribute to their cytotoxic effects against cancer cells. This approach enhances our understanding of the molecular mechanisms underpinning the anticancer activity of TMESLR and underscores their therapeutic potential.

In order to build the Protein-Protein Interaction (PPI) network for this investigation, the STRING database was used (accessed on Sep. 10, 2024), version 12.0 (https://string-db.org/), to examine proteins associated with cancer pathways and the bioactive chemicals found in the TMESLR. This analysis enabled the identification of direct and functional associations between the selected proteins and compounds. The resulting PPI network was visualized using Cytoscape software, version 3.10.1, allowing for comprehensive exploration of the interactions. The Cytoscape analyzer tool was utilized to generate a detailed interaction network consisting of 67 nodes and 1306 connections, with an average node connectivity of 38.98 (Supplemental Figure S1). This network provides a deeper understanding of the complex interplay between bioactive compounds and protein targets, revealing potential pathways involved in the cytotoxic activities of TMESLR.

Identification of Key Hub Genes in the PPI Network. Important hub genes in the PPI network linked to the anticancer properties of TMESLR compounds were found using the CytoHubba plugin. The highly connected hub genes include CASP3, CASP8, CASP9, FADD, BCL2, BCL2L1, CYCS, APAF1, TNF, FASLG, and XIAP, which are central to apoptosis regulation and cancer cell signaling pathways Figure 7. These genes represent potential molecular targets and provide valuable insights into the mechanisms driving the cytotoxic effects of the bioactive compounds. Their strong connectivity in the network underscores their significance in mediating the therapeutic potential of the compounds.

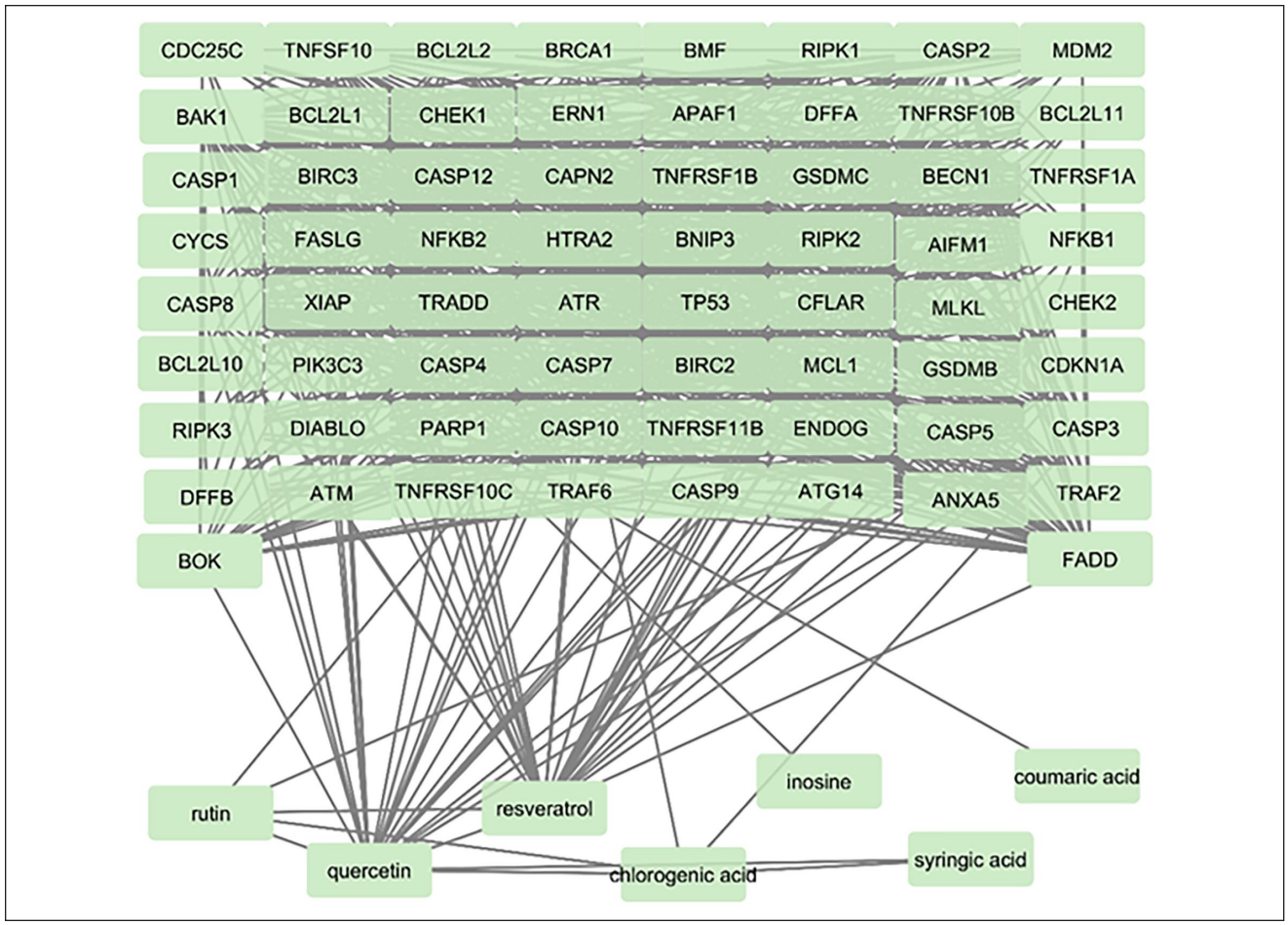

Figure 6. STITCH analysis illustrating the interactions between key protein targets associated with cancer and the principal bioactive compounds identified in the TMESLR.

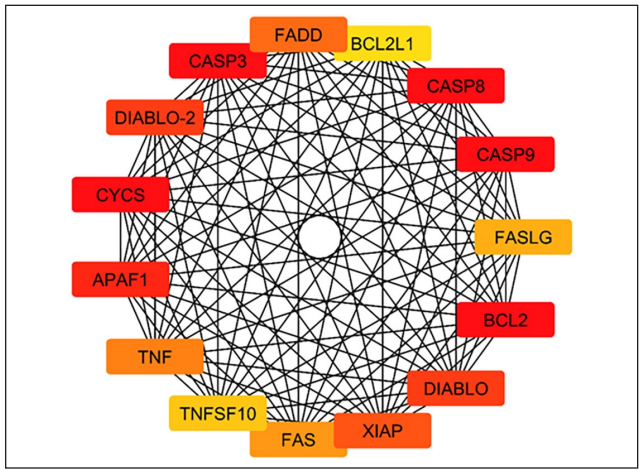

Figure 7. Key hub genes identified in the PPI network related to the anticancer activity of TMESLR compounds. The highlighted genes, including CASP3, CASP8, CASP9, FADD, BCL2, BCL2L1, CYCS, APAF1, TNF, FASLG, and XIAP, play critical roles in apoptosis and cancer-related signaling pathways, emphasizing their importance as central nodes in the interaction network.

Analysis of Overrepresented Gene Ontology (GO) Terms. GO enrichment study for the current study on the anticancer properties of TMESLR compounds was accompanied using ShinyGO v0.80. Our results highlight the main protein involvement across key categories Figure 8, providing insights into their functional roles in cancer-related pathways. Apoptotic processes, the control of apoptosis-related cysteine-type endopeptidase activity, intrinsic apoptotic signaling pathways, and the activation of apoptotic signaling through death domain receptors are among the enriched GO items in the BP category. Other notable terms involve the positive regulation of cytochrome c release from mitochondria and the regulation of necroptosis and autophagy. These findings indicate that the bioactive compounds are heavily involved in processes central to the induction of apoptosis and cancer cell death mechanisms, underscoring their therapeutic potential. In the CC category, significant GO terms include the death-inducing signaling complex, caspase complex, apoptosome, ripoptosome, and the CD95 death-inducing signaling complex. Additional terms such as the tumor necrosis factor receptor superfamily complex,

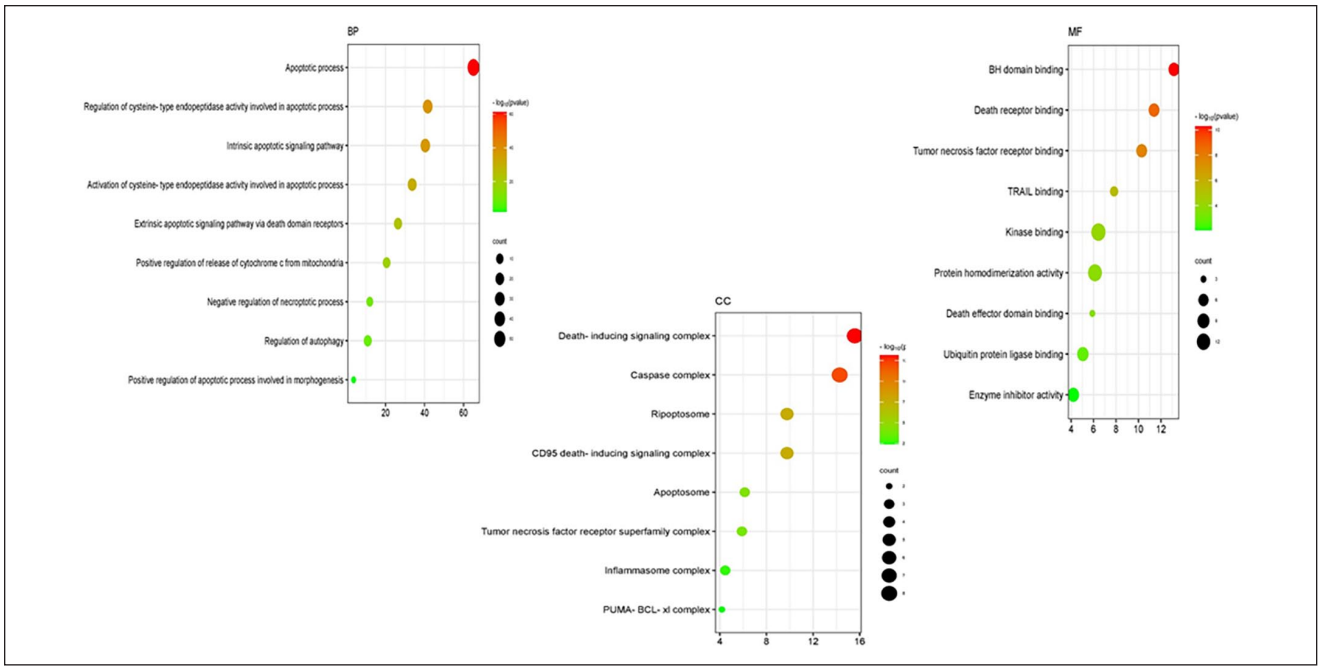

Figure 8. The Gene Ontology (GO) classifications for the anticancer properties of compounds found in TMESLR are depicted in a bubble chart. The enriched categories Biological Processes (BP), Cellular Components (CC), and Molecular Functions (MF) are highlighted in the chart, with particular attention paid to their roles in apoptosis, signaling cascades, and protein interactions that are essential for cancer treatment.

and inflammasome complex highlight the involvement of these proteins in apoptotic and inflammatory signaling. These cellular locations suggest that the compounds target critical components within signaling complexes, leading to the activation of programed cell death, and immune-modulatory effects. For the MF category, enriched terms include BH domain binding, death receptor binding, tumor necrosis factor receptor binding, TRAIL binding, and kinase binding. Additionally, terms such as protein homodimerization activity, ubiquitin-protein ligase binding, and enzyme inhibitor action were recognized. These molecular functions propose that the compounds exert their effects through interactions with receptors, and enzymes critical for cancer cell survival, and apoptosis regulation. This comprehensive GO analysis reveals that TMESLR compounds target multiple pathways, and mechanisms central to cancer progression, highlighting their potential as multifunctional therapeutic agents. The visualized data provide a deeper understanding of their molecular roles, and possible applications in anticancer therapy.

Examination of Predominant KEGG Pathways. The KEGG pathway analysis conducted in the present study highlights the molecular mechanisms by which the bioactive compounds from TMESLR exerts anticancer effects. The results are visualized in Figure 9, reveal important enhancement in key pathways such as apoptosis, the p53 signaling pathway, TNF signaling, NF-kappa B signaling, and necroptosis. These pathways are central to cancer progression, and cell survival, illustrating the ability of the bioactive compounds to regulate apoptotic mechanisms, and disrupt cancer cell proliferation. Additionally, pathways associated with drug resistance (eg, platinum drug resistance), and specific cancer types (eg, small cell lung cancer) were notably enriched, suggesting the therapeutic potential of these compounds. This analysis provides a comprehensive understanding of the targeted pathways, offering insights into how TMESLR compounds interact with molecular networks.

Molecular Modeling With Human HDAC2. Human Histone Deacetylase 2 (HDAC2) is a crucial enzyme implicated in the regulation of gene expression, and epigenetic modifications. Its overexpression has been linked to the development, and progression of various cancers, including Caco-2, MCF-7, and HepG2.[45-47] Targeting HDAC2 can restore normal acetylation levels, leading to cell cycle arrest, apoptosis, and reduced cancer cell proliferation.[48] This makes HDAC2 a promising therapeutic target for developing effective anticancer agents. In this study, molecular docking simulations were performed to evaluate the interaction of compounds derived from TMESLR (**1-17**) with Human HDAC2. SAHA (Vorinostat®), a well-known HDAC inhibitor, was used as a reference ligand.[49] The crystal structure of HDAC2 (PDB ID: 4LXZ) was

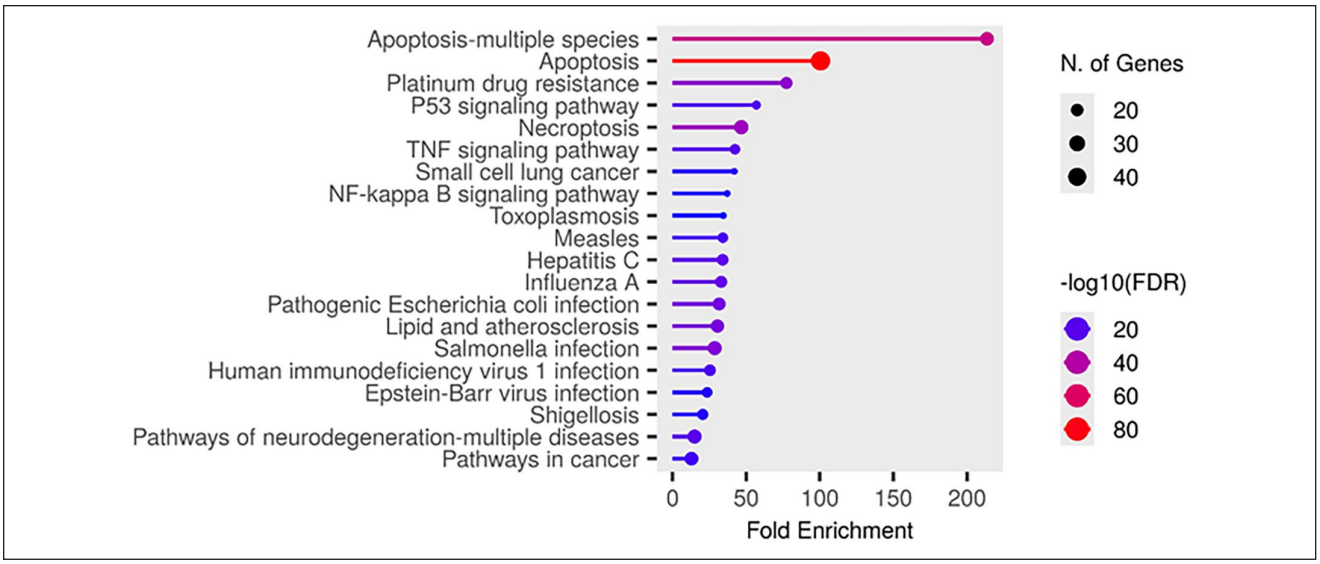

Figure 9. Bar plot illustrating the significantly enriched KEGG pathways targeted by TMESLR compounds, highlighting their potential anticancer effects. The pathways include apoptosis, p53 signaling, TNF signaling, and NF-kappa B signaling, showcasing the role in disrupting cancer progression and promoting therapeutic outcomes.

retrieved from the RCSB Protein Data Bank.[50] To evaluate these compounds' binding affinities, and interaction profiles with the HDAC2 active site, docking simulations were performed. The findings are described in detail in Supplemental Table S3. Among the studied compounds, inosine (**6**), and chlorogenic acid (**12**) emerged as the most promising choices, displaying substantial binding affinity, low RMSD value, and significant interactions with key residues. These criteria jointly define their potential as effective inhibitors. **Inosine** (**6**) presented a docking score of −7.86 kcal/mol with an RMSD value of 0.90. The 3D structure of inosine docked into the HDAC2 active site Figure 10 shows multiple interactions with critical residues, including **GLY154, TYR308, ASP269, HIS146, and ASP181**, which play essential roles in enzyme activity, and inhibition. These interactions stabilize the binding of inosine, making it a promising candidate for anticancer applications. The 2D interaction map Figure 10 further details the specific types of interactions. **Conventional hydrogen bonds** are observed with TYR308, and ASP269, while **Pi-Stacked interactions** and **van der Waals forces** enhance the affinity, and stability within the binding pocket. The detailed visualization highlights the molecular precision with which inosine interacts with HDAC2, providing a clear framework for its inhibitory potential. Similarly, **chlorogenic acid** (**12**) demonstrated a notable docking score of −7.32 kcal/mol and an RMSD value of 1.44. The 3D structure Figure 10 of chlorogenic acid within the HDAC2 binding pocket reveals interactions with critical residues, including **TYR308, PHE210, PRO34, LEU276, and PHE155**. These interactions are essential for inhibiting HDAC2 activity, and indicating the strong potential as an anticancer agent. The 2D interaction map Figure 10 further delineates the specific interactions of chlorogenic acid. **Conventional hydrogen bonds** are formed with TYR308, and PHE210, while **van der Waals forces** and **Pi-Alkyl interactions** enhance the stability of the compound within the active site. These interactions collectively contribute to chlorogenic acid's strong binding affinity, as reflected by its docking score and low RMSD value. In comparison, the reference ligand SAHA depicted a docking score of −7.01 kcal/mol and an RMSD value of 1.75. Although, it shared several interaction sites, such as TYR308, PHE155, ASP269, and HIS146, with TMESLR compounds, inosine and chlorogenic acid exhibited stronger binding affinities, suggesting their superior potential as HDAC2 inhibitors. These findings highlight the potential of TMESLR compounds to inhibit HDAC2 activity effectively. By disrupting HDAC2 function, these compounds can induce apoptosis and suppress cancer cell proliferation in Caco-2, MCF-7, and HepG2 cell lines. This study provides a foundation for further exploration of TMESLR compounds as therapeutic agents in cancer treatment.

Discussion

Prior research showed that the ethanol extract of *S. lycopersicum* fruits exhibited an antiproliferative effect against HepG2 cell line with an IC_{50} value of 48.0 µg/mL.[51] The present study reveals, for the first time, the significant in vitro cytotoxic activity of the waste product, *S. lycopersicum* roots, against the cancer cell lines Caco-2, MCF-7, and HepG2.

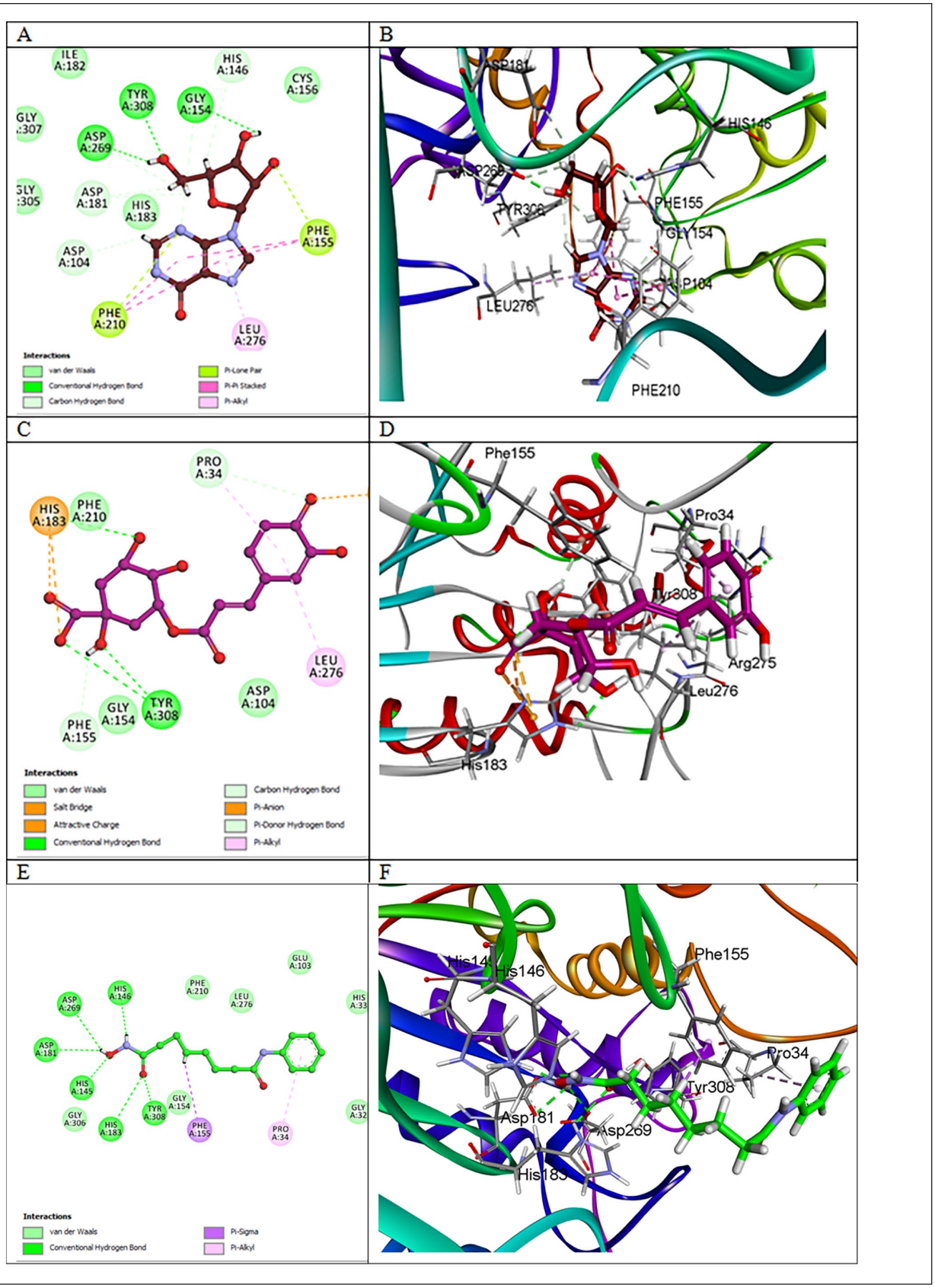

Figure 10. Binding interactions with Human HDAC2. (A and B) Interaction maps of inosine (**6**). (C and D) Interaction maps of chlorogenic acid (**12**). (E and F) Interaction map of reference ligand SAHA (Vorinostat®).

Interestingly, our results evidenced that the prepared TMESLR-NCs notably enhanced the cytotoxic activity of TMESLR, particularly against Caco-2 (41%) and HepG2 (16%) cancer cell lines. A result that indicates the cytotoxic potential of such an ignored plant part, commonly considered as a vegetable waste product.

LC-MS metabolomic analysis characterized the presence of various chemical classes in the studied extract, including flavonoids, terpenes, ionones, and phenolic acids are illustrated in Supplemental Table S1 and Figure 3. This metabolic profile distinctly explicated the cytotoxic potential of TMESLR. For instance, phytol (**7**),[52] inosine (**6**),[33] rutin (**17**),[53] resveratrol (**4**)[54] and chlorogenic acid (**12**)[55] have all been previously reported to exert notable cytotoxic effects.

TMESLR and its prepared-NCs demonstrated significant cytotoxic effects, involvement in apoptosis-related pathways, and strong interactions with key proteins like HDAC2.[56] The identification of hub genes such as CASP3, BCL2, and TNF, along with enriched pathways including apoptosis and p53 signaling, highlights their molecular mechanisms of action.[57] Molecular docking results further confirm the promising role of inosine (**6**) and chlorogenic acid (**12**)[12] as HDAC2 inhibitors, capable of disrupting cancer progression and inducing apoptosis.[58] These findings place TMESLR and TMESLR-NCs as promising candidates for future anticancer therapies.

Conclusions

The findings of this study revealed that the TMESLR revealed significant cytotoxicity against Caco-2, MCF-7, and HepG2 cells. Also, TMESLR-NCs displayed superior cytotoxic activity, particularly against Caco-2 and HepG2 cancer cell lines. Metabolomic profiling using LC-MS metabolomic analysis identified **17** secondary metabolites from various chemical classes in TMESLR. *In silico* studies, including PPI network analysis, GO enrichment analysis, and molecular docking simulations, provided valuable insights into the potential mechanisms underlying the anticancer activity of TMESLR compounds. The PPI network revealed key hub genes such as CASP3, BCL2, and TNF, which are central to apoptosis and cancer signaling pathways. GO enrichment analysis highlighted the overrepresentation of terms associated with apoptosis, cell death regulation, and immune response. Molecular docking study suggested that inosine and chlorogenic acid bind strongly to Human Histone Deacetylase 2 (HDAC2), a vital target in cancer progression. These findings highlight the potential of TMESLR and TMESLR-NCs as promising candidates for the development of novel anticancer agents. Further investigations are warranted to explore the *in vivo* efficacy of TMESLR and TMESLR-NCs in preclinical animal models of cancer to confirm their therapeutic potential.

Author Contributions

Marwa A. M. Abdelrazek and Miada F. Abdelwahab: writing original draft, visualization, validation, investigation, formal analysis, and data curation. Soad A. Mohamed: methodology, and conceptualization. Hesham A. Abo Zeid: validation, software, methodology, and conceptualization. Usama R. Abdelmohsen and Ashraf N. E. Hamed: reviewing, supervision, methodology, investigation, data curation, and conceptualization.

Funding

The author(s) received no financial support for the research, authorship, and/or publication of this article.

Declaration of conflicting interests

The author(s) declared no potential conflicts of interest with respect to the research, authorship, and/or publication of this article.

Data availability statement

This article and its supplemental information files contain all of the data generated during this investigation.

Supplemental Material

Supplemental material for this article is available online.

References

1. Siegel RL, Miller KD, Fuchs HE, et al. Cancer statistics. *CA Cancer J Clin*. 2022;72(1):7-28. doi:10.3322/caac.21442
2. Sarris M, Nikolaou K, Talianidis I. Context-specific regulation of cancer epigenomes by histone and transcription factor methylation. *Oncogene*. 2014;33(10):1207-1217. doi:10.1038/onc.2013.87
3. Sarris ME, Moulos P, Haroniti A, et al. Smyd3 is a transcriptional potentiator of multiple cancer-promoting genes and required for liver and colon cancer development. *Cancer Cell*. 2016;29(3):354-366. doi:10.1016/j.ccell.2016.01.013
4. Goel H, Siddiqui L, Mahtab A, et al. Fabrication design, process technologies, and convolutions in the scale-up of nanotherapeutic delivery systems. *Nanotube Ther*. 2022;2022:47-131. doi:10.1016/B978-0-12-820757-4.00017-X
5. Rao CNR, Thomas PJ, Kulkarni GU. *Nanocrystals: Synthesis, Properties and Applications*. Springer Science + Business Media; 2007;25-68.
6. Hanutami NPB, Budiman A. Article Review: The Use of Nanotechnology in Herbal Medicine Formulation. Farmaka (Medicines). 2017;15(2):29-41. doi:10.24198/JF.V15I2.12947
7. Joseph E, Singhvi G. Multifunctional nanocrystals for cancer therapy: a potential nanocarrier. *Nanomater. Drug Deliv. Ther*. 2019;2019:91-116. doi:10.1016/B978-0-12-816505-8.00007-2
8. Abushammala H. On the para/ortho reactivity of isocyanate groups during the carbamation of cellulose nanocrystals using 2, 4-toluene diisocyanate. *Polymers*. 2019;11(7):1164. doi:10.3390/polym11071164
9. Samiei M, Moghaddam FA, Abdolahinia ED, et al. Influence of curcumin nanocrystals on the early osteogenic

differentiation and proliferation of dental pulp stem cells. *Nanomater*. 2022;2022:1-8. doi:10.1155/2022/8517543
10. Jahangir MA, Imam SS, Muheem A, et al. Nanocrystals: characterization overview, applications in drug delivery, and their toxicity concerns. *J Pharm Innov*. 2022;17:237-248. doi:10.1007/s12247-020-09499-1
11. Elmaidomy AH, El Zawily A, Salem AK, et al. New cytotoxic dammarane type saponins from *Ziziphus spina-christi*. *Sci Rep*. 2023;13(1):20612. doi:10.1038/s41598-023-46841-2
12. Mohammed MHH, Hamed ANE, Elhabal SF, et al. Metabolic profiling and cytotoxic activities of ethanol extract of *Dypsis leptocheilos* aerial parts and its green synthesized silver nanoparticles supported by network pharmacology analysis. *S Afr J Bot*. 2023;161:648-665. doi:10.1016/j.sajb-2023-08-026
13. Ahmed SST, Fahim JR, Youssif KA, et al. Metabolomics of the secondary metabolites of *Ammi visnaga* L. roots (family Apiaceae) and evaluation of their biological potential. *S Afr J Bot*. 2022;149:860-869. doi:10.1016/j.sajb-2022-01-011
14. El-Hawwary SS, Saber FR, Abd Almaksoud HM, et al. Cytotoxic potential of three Sabal species grown in Egypt: a metabolomic and docking-based study. *Nat Prod Res*. 2022;36(4):1109-1114. doi:10.1080/14786419-2020-1851228
15. Koparde AA, Doijad RC, Magdum CS. Natural products in drug discovery. In: Perveen S, Al-Taweel A (eds) *Pharmacognosy-Medicinal Plants*. IntechOpen; 2019; Chapter 14, 269-270. doi: 10.5772-intechopen-81860
16. Gerszberg A, Hnatuszko-Konka K, Kowalczyk T, et al. Tomato (*Solanum lycopersicum* L.) in the service of biotechnology. *Plant Cell Tissue Organ Cult*. 2015;120:881-902. doi:10.1007/s11240-014-0664-4
17. Hamed ANE, Abdelaty NA, Attia EZ, et al. Antiproliferative potential of *Moluccella laevis* L. aerial parts family Lamiaceae (Labiatae), supported by phytochemical investigation and molecular docking study. *Nat Prod Res*. 2022;36:1391-1395. doi:10.1080/14786419-2021-1876046
18. Mosmann T. Rapid colorimetric assay for cellular growth and survival: application to proliferation and cytotoxicity assays. *J Immunol Methods*. 1983;65(1-2):55-63. doi:10.1016/0022-1759(83)90303-4
19. Zahran EZ, Mohamad SA, Yahia R, et al. Anti-otomycotic potential of nanoparticles of *Moringa oleifera* leaf extract: an integrated *in vitro*, *in silico* and phase 0 clinical study. *Food Funct*. 2022;13(21):11083-11096. doi: 10.1039/d2fo02382b
20. Saah S, Kaewkroek K, Wiwattanapatapee R. Cytotoxic effect of surfactants used in self-microemulsifying drug delivery systems (SMEDDS) on normal and cancer gastrointestinal cell lines. *Lat Am J Pharm*. 2018;37(11):2244-2253.
21. DNP: Dictionary of Natural Products. Accessed September 13, 2020. http://dnp.chemnetbase.com/faces/chemical/ChemicalSearch.xhtml.
22. METLIN. Metabolomic Databases, Accessed September 1, 2020. http://metlin.scripps.edu/index.php.
23. Dany F, Nikmah UA, Lienggonegoro LA. Critical response to article network pharmacology and experimental validation to explore the effect and mechanism of kanglaite injection against triple-negative breast cancer. *Drug Des Devel Ther*. 2023;17:2455-2456. doi:10.2147/DDDT.S417549
24. Zhou Y, Wu Q, Wang X, et al. Insights into the functional mechanism of diabetic kidney disease treatment with sinensetin based on network pharmacology and molecular docking. *Integr Med Nephrol Androl*. 2023;10(4):e00033. doi:10.1097/IMNA-D-22-00033
25. Szklarczyk D, Kirsch R, Koutrouli M, et al. The STRING database in 2023: protein-protein association networks and functional enrichment analyses for any sequenced genome of interest. *Nucleic Acids Res*. 2023;51(D1):D638-D646. doi:10.1093/nar/gkac1000
26. Ma H, He Z, Chen J, et al. Identifying of biomarkers associated with gastric cancer based on 11 topological analysis methods of CytoHubba. *Sci Rep*. 2021;11(1):1331. doi: s41598-020-79235-9
27. Karoii DH, Azizi H, Skutella T. Integrating microarray data and single-cell RNA-Seq reveals key gene involved in spermatogonia stem cell aging. *Int J Mol Sci*. 2024;25(21):11653. doi:10.3390/ijms252111653
28. Tang D, Chen M, Huang X, et al. SRplot: a free online platform for data visualization and graphing. *PLoS One*. 2023;18(11):e0294236. doi:10.1371/journal.pone.0294236
29. Parween A, Singh PK, Anamika Y. Molecular docking of quinolone against INHA to treat tuberculosis. *Int J Res Appl Sci Eng Technol*. 2020;8(VI):2421-2427. doi: 10.22214/ijraset.2020.6389
30. Kakran M, Shegokar R, Sahoo NG, et al. Long-term stability of quercetin nanocrystals prepared by different methods. *J Pharm Pharmacol*. 2012;64(10):1394-1402. doi:10.1111/j.2042-7158-2012-01515-x
31. Yadi M, Mostafavi E, Saleh B, et al. Current developments in green synthesis of metallic nanoparticles using plant extracts: a review. *Artif Cells Nanomed Biotechnol*. 2018;46(3):S336-S343. doi:10.1080/21691401-2018-1492931
32. Bohlouli S, Jafarmadar Gharehbagh F, Dalir Abdolahinia E, et al. Preparation, characterization, and evaluation of rutin nanocrystals as an anticancer agent against head and neck squamous cell carcinoma cell line. *Nanomater*. 2021;2021:1-8. doi:10.1155/2021/9980451
33. Kumar M, Tomar M, Bhuyan DJ, et al. Tomato (*Solanum lycopersicum* L.) seed: A review on bioactives and biomedical activities. *Biomed Pharmacother*. 2021;142:112018. doi:10.1016/j.biopha.2021.112018
34. Flores IR, Vásquez-Murrieta MS, Franco-Hernández MO, et al. Bioactive compounds in tomato (*Solanum lycopersicum*) variety saladette and their relationship with soil mineral content. *Food Chem*. 2021;344:128608. doi:10.1016/j.foodchem.2020.128608
35. Cheng G, Chang P, Shen Y, et al. Comparing the flavor characteristics of 71 tomato (*Solanum lycopersicum*) accessions in central Shaanxi. *Front Plant Sci*. 2020;11:586834. doi:10.3389/fpls.2020.586834
36. Nityasree BR, Chalannavar RK, Ghosh SK, Divakar MS, Sowmyashree K. Effect of *Solanum lycopersicum* leaf extracts against larvicidal activity of *Aedes aegypti* L. *BioMedicine*. 2020;40(4):467-473. doi: 10.51248/.v40i4.321
37. Seong SH, Jung HA, Choi JS. Discovery of flazin, an alkaloid isolated from cherry tomato juice, as a novel non-enzymatic protein glycation inhibitor via *in vitro* and *in silico* studies. *J Agric Food Chem*. 2021;69(12):3647-3657. doi:10.1021/acs.jafc.0c07486

38. Olsen KM, Hehn A, Jugdé H, et al. Identification and characterisation of CYP75A31, a new flavonoid 3'5'-hydroxylase, isolated from *Solanum lycopersicum. BMC Plant Biol*. 2010;10(1):21. doi:10.1186/1471-2229-10-21
39. Lima TSP, Borges MM, Buarque FS, et al. Purification of vitamins from tomatoes (*Solanum lycopersicum*) using ethanolic two-phases systems based on ionic liquids and polypropylene glycol. *Fluid Phase Equilib*. 2022;557:113434. doi:10.1016/j.fluid.2022.113434
40. Edgar R, Domrachev M, Lash AE. Lash, Gene Expression Omnibus: NCBI gene expression and hybridization array data repository. *Nucleic Acids Res*. 2002;30(1):207-210. doi:10.1093/nar/30.1.207
41. Whirl-Carrillo M, Huddart R, Gong L, et al. An evidence-based framework for evaluating pharmacogenomics knowledge for personalized medicine. *Clin Pharmacol Ther*. 2021;110(3):563-572. doi: 10.1002/cpt.2350
42. Ritchie ME, Phipson B, Wu D, et al. Limma powers differential expression analyses for RNA-sequencing and microarray studies. *Nucleic Acids Res*. 2015;43(7):e47-e47. doi:10.1093/nar/gkv007
43. Szklarczyk D, Gable AL, Nastou KC, et al. The STRING database in 2021: customizable protein–protein networks, and functional characterization of user-uploaded gene/measurement sets. *Nucleic Acids Res*. 2021;49(D1):D605-D612. doi:10.1093/nar/gkaa1074
44. Kanehisa M, Furumichi M, Tanabe M, et al. KEGG: new perspectives on genomes, pathways, diseases and drugs. *Nucleic Acids Res*. 2017;45(D1):D353-D361. doi:10.1093/nar/gkw1092
45. Shukla P, Bajpai K, Tripathi S, et al. A review on the taxonomy, ethnobotany, chemistry and pharmacology of *Solanum lycopersicum* Linn. *Int J Chem Pharm Sci*. 2013;1(8):521-527.
46. Garmpis N, Damaskos C, Dimitroulis D, et al. Clinical significance of the histone deacetylase 2 (HDAC-2) expression in human breast cancer. *J Pers Med*. 2022;12(10):1672. doi:10.3390/jpm12101672
47. Liu YR, Wang JQ, Huang ZG, et al. Histone deacetylase-2: a potential regulator and therapeutic target in liver disease. *Inter J Molecular Med*. 2021;48(1):131. doi:10.3892/ijmm.2021.4964
48. Conte M, Di Mauro A, Capasso L, et al. Targeting HDAC2-mediated immune regulation to overcome therapeutic resistance in mutant colorectal cancer. *Cancers* (Basel). 2023;15(7):1960. doi:10.3390/cancers15071960
49. Mehmood SA, Sahu KK, Sengupta S, et al. Recent advancement of HDAC inhibitors against breast cancer. *Med Oncol*. 2023;40(7):201. doi:10.1007/s12032-023-02058-x
50. Anand A, Ghosh P, Singh R, et al. Identification of potent histone deacetylase 2 (HDAC2) inhibitors through combined structure and ligand-based designs and molecular modelling approach. *J Biomol Struct Dyn*. 2024;42(9):4679-4698. doi:10.1080/07391102.2023.2222177
51. Mutalib MA, Shamsuddin AS, Ramli NNN, et al. Antiproliferative activity and polyphenol analysis in tomato (*Solanum lycopersicon*). *Malays J Microsc*. 2023;19(1):282-294.
52. Shariare MH, Noor HB, Khan JH, et al. Liposomal drug delivery of *Corchorus olitorius* leaf extract containing phytol using design of experiment (DoE): in-vitro anticancer and *in-vivo* anti-inflammatory studies. *Colloids Surf B Biointerfaces*. 2021;199:111543. doi:10.1016/j.colsurfb.2020.111543
53. Caparica R, Júlio A, Araújo MEM, et al. Anticancer activity of rutin and its combination with ionic liquids on renal cells. *Biomolecules*. 2020;10(2):233. doi:10.3390/biom10020233
54. Soo E, Thakur S, Qu Z, et al. Enhancing delivery and cytotoxicity of resveratrol through a dual nanoencapsulation approach. *J Colloid Interface Sci*. 2016;462:368-374. doi:10.1016/j.jcis.2015.10.022
55. Hernandes LC, Machado ART, Tuttis K, et al. Caffeic acid and chlorogenic acid cytotoxicity, genotoxicity and impact on global DNA methylation in human leukemic cell lines. *Genet Mol Biol*. 2020;43(3):e20190347. doi:10.1590/1678-4685-GMB-2019-0347
56. Jo H, Shim K, Kim HU, et al. HDAC2 as a target for developing anti-cancer drugs. *Comput Struct Biotechnol J*. 2023;21:2048-2057. doi:10.1016/j.csbj.2023.03.016
57. Mohammed MHH, Hamed ANE, Elhabal SF, et al. Chemical composition and anti-proliferative activities of *Hyophorbe lagenicaulis* aerial parts and their biogenic nanoparticles supported by network pharmacology study. *S Afr J Bot*. 2023;156:398-410. doi:10.1016/j.sajb.2023.03.018
58. Mohammed MHH, Hamed ANE, Sayed AM, et al. Antiproliferative potential of *Dypsis decaryi* seeds supported by metabolic profiling and molecular docking. *J Herb Med*. 2024;44:100846. doi:10.1016/j.hermed.2024.100846